

SLAC-PUB-3645
SLAC/AP-42
April 1985
(A/AP)

Higher Luminosities via Alternative Incident Channels*

J. E. Spencer
Stanford Linear Accelerator Center
Stanford University, Stanford, CA 94305

1. Prologue

When Ben Johnson was asked, *"What is Poetry?"* he replied: *"Why Sir, it is much easier to say what it is not. We all know what light is; but it is not easy to tell what it is."* Nevertheless, according to Einstein: *"Most of the fundamental ideas of science are essentially simple, and may, as a rule, be expressed in a language comprehensible to everyone."* Of course, some effort is necessary before reconciling this comment with another by Einstein: *"For an idea that does not at first seem insane, there is no hope."* These comments seem especially appropriate for colliding beam physics where the basic ideas are simple enough but their technical realization ranges from difficult to impossible. Consistent with this tradition, we show that PEP provides some unique opportunities for one and two photon physics with real photons as well as for QCD studies with internal targets. Photon beams would avoid the major limitation on the luminosity of present machines and could provide PEP an ideal b-physics factory producing the full range of J_c^{PC} and J_b^{PC} states that may not be observable otherwise as well as allow a whole new class of "missing-mass" experiments. These latter particles are the pseudo-Goldstone bosons and their supersymmetric counterparts. These and related possibilities like a single-pass, "free electron laser" facility or even synchrotron radiation beam lines all favor a mini-maxi configuration for the low-beta insertions in PEP. This allows more diverse experiments without excluding any ongoing experimental programs. Such possibilities have interesting implications for a number of proposed facilities including the SSC. Some systematic machine physics studies over a range of energies are suggested.

* Work supported by the Department of Energy, contract DE-AC03-76SF00515.

2. Some History and Perspective

In a sense, the SLAC linac was built to provide highly space-like photons¹ for deep inelastic scattering experiments on few-nucleon systems. Such experiments demonstrated the basic underlying parton structure of the nucleon. In direct contrast, the subsequent development of SPEAR provided highly time-like photons via the (e^+, e^-) annihilation process shown in Fig. 1b. This led to the "November Revolution" based on the first observations of resonant production of charmed quark pairs (q_c, \bar{q}_c) as well as the heavy, electron-like particle called the tau. These are still interesting and productive fields of research at SPEAR.

With the higher energies available at PEP, higher-order processes become important with the space-like photon production processes of Fig. 1c being dominant. This two photon reaction is the main production channel for C-even particles with the physics of interest at the internal vertices in diagrams such as Fig. 1f where $X \equiv f\bar{f}$. Because there are two virtual photons, this process lacks the simplicity of the annihilation diagram of Fig. 1b but, as Brodsky has made clear, is really more interesting because of the different types of experiments that occur depending on whether the photons are almost real or far off the mass shell. The situation again simplifies when Fig.'s 1f or 1g become the incident channel producing η_b 's, A_{2b} 's, A_{3b} 's ... etc.

The present proposal considers using real photons that are on the light-cone or light-like such as shown in Figures d-h. The basic idea resulted from a study related to the SLC more than five years ago² in which the motivation was to provide more than the one (e^+, e^-) interaction region by also allowing for (e^-, e^-) , (e^-, γ) , (e^+, γ) and (γ, γ) channels. This was to be done by either increasing the number of bunches in a beam and/or using multiple traversals of the ring by adding RF. For instance, one could use 3 or 4 electron bunches (without any e^+ bunches) to study: W's rather than Z's via $\gamma e^\pm \rightarrow \nu W^\pm$ as shown in Fig. 1d; Higgs, axions or other pseudo-Goldstone bosons via $\gamma\gamma \rightarrow H^0 (J^{PC} = 0^{++})$ or $a^0 (J^{PC} = 0^{-+})$ as shown in Fig. 1g; or possibly explore composite electron models such as suggested by Harari³ through $e^-e^- \rightarrow \mu^-e^-, \tau^-e^-, etc.$ or more simply through $\gamma e \rightarrow e^*$ via diagrams 1d or 1e as in various low energy photophysics studies but with high energy, real, polarized photons.

¹ I assume the natural metric for four-vectors with $p \equiv (\epsilon, i\vec{p})$ and $\hbar = c = 1$ so $s = (\omega_1 + \omega_2)^2 - (\vec{k}_1 + \vec{k}_2)^2 \equiv 4\omega_1\omega_2$ for collinear collisions between real photons.

² J. E. Spencer, SLAC-PUB-2677, Feb. 1981; see also C. Akerlof, SLC Workshop Notes Sept. 1981; I.F. Ginzburg, G. L. Kotkin, V. G. Serbo and V. I. Telnov, Pisma ZHETF **34**, Nov. 1981, 514.

³ H. Harari, Proc. 8th and 10th SLAC Summer Inst., SLAC-REP-239 (1981).

Further, if the virtual fermion in Fig. 1f is considered to be a supersymmetric particle such as a photino, then other sparticles will be produced such as a pair of goldstinos. Such uncharged, possibly light mass fermions as the goldstino or photino are reminiscent of neutrinos and like their boson counterparts provide candidates for the cosmological missing-mass. In present setups, these experiments would require double tagging with a signature of $\gamma^*\gamma^* \rightarrow \text{nothing}$ rather than e.g. an anomaly in the $\gamma\gamma$ scattering cross section. Perhaps the best historical precedent for this kind of experiment is the pion which is a pseudo-Goldstone boson that took 14 years to find.

One problem of concern in the SLC study was the loss of C-M energy when using lasers to Compton convert the particle beam to photons. While lasers could probably be made to convert the electron beam with good efficiency, one would lose too much C-M energy to produce intermediate vector bosons². Free electron lasers could provide limited variability, but probably couldn't provide enough intensity at the desired photon energy. Such considerations are less relevant for PEP which can be used in conjunction with a higher energy, lower emittance linac beam to Compton convert a low energy, high intensity, monochromatic photon beam. The latter can be produced using a high current density PEP bunch with a wiggler in a coherent way. From classical arguments², one expected monochromatic photons up to 1 MeV in the primary photon beam produced from the SLC bunch but with too low gain i.e. $\alpha N_e (\lambda_\gamma / 10\sigma_e) \lesssim 5 \times 10^5 \alpha$ photons per electron for $\omega_\gamma = 10$ eV without microbunching based on the usual assumptions for the SLC current and bunch length. With self bunching or that induced by an external laser, the limit approaches $0.5 N_e \alpha$ (assuming a pure fundamental) for sufficiently low photon energies. This subject is resurrected for storage rings with PEP as example.

Using high current, stored bunches to produce the primary photon beam which is Compton converted to high energy by backscattering on a high current, high energy linac beam appears to be an excellent way to upgrade the effective energy and luminosity of existing storage rings. The energy is increased by using an upgraded linac beam and real photons and the reaction rates are improved because photoproduction cross sections are larger than electroproduction and higher current densities are possible by eliminating the conventional beam-beam interaction. These points are discussed in succeeding sections and illustrated with several examples of different incident channels: 1) e- γ , 2) γ - γ , and 3) e-A and γ -A scattering and reactions. Such experiments need not exclude one another nor any on-going experimental programs. Furthermore, the primary photon beam would be a significant new research and development tool for synchrotron radiation users.

3. Luminosity Limitations

Designing storage rings for a specific process in Fig. 1 might emphasize energy spread for Fig. 1b and electron polarization for Fig. 1c but the most important parameters characterizing both accelerators and storage rings are the energy range (C-M) and the beam current or luminosity available over this range. While the primary goal is to reach higher energies, it also seems important to improve the luminosity and range of capabilities of existing facilities. The PEP storage ring, with its large, single-beam energy range ($E_b \sim 4 - 18\text{GeV}$) in conjunction with the SLAC high energy, high current, low emittance linac beam provides some unique opportunities to overcome a fundamental limitation on the luminosity of colliding beam machines.

The incoherent beam-beam interaction between colliding bunches produces strong, **nonlinear** forces on the bunches which limit the operation of present rings. The leading-order, linear focusing force for head-on e^\pm collisions, expressed as a tune perturbation per crossing, is⁴

$$\Delta\nu_{x,y} = \frac{r_e N_e \beta_{x,y}^*}{2\pi\gamma\sigma_{x,y}^*(\sigma_x^* + \sigma_y^*)}$$

where σ is the rms bunch size, N_e is the number of particles per bunch and β^* is the beta function at the crossing point or IR. Although this expression can be identified with the average, small amplitude tune shift for gaussian bunches it is best thought of as the tune *spread* in the core of the bunch. At some limiting value of this tune spread ($\Delta\nu^*$) or bunch current (N_e^*) the bunch cross-section increases, luminosity fails to increase and may decrease and the lifetime may also decrease. If this limit is made the same in both transverse directions by making $\beta_y^*/\beta_x^* \simeq K (\equiv \epsilon_y/\epsilon_x, \text{ the tune independent, x-y coupling in the machine})$, one expects the maximum achievable luminosity for $\sigma_x \gg \sigma_y$ to be:

$$\mathcal{L}_{max} = \frac{(N_e^*)^2}{4\pi\sigma_x^*\sigma_y^*} f n = (\Delta\nu^*)^2 \left(\frac{\gamma}{r_e}\right)^2 \frac{\epsilon_x}{\beta_y^*} f n$$

where $\epsilon_x = \pi\sigma_x^2/\beta_x$, f is the revolution frequency and n is the number of bunches per beam. Table II for PEP and SPEAR shows they are both near their limits of $10^{31} < \mathcal{L} < 10^{32}$.

⁴ M. Sands, SLAC-121, 1970. For protons one should use the classical proton radius, r_p . For internal targets, this should be negligible with an ion clearing field

Increasing the frequency via superconducting magnets, or the number of bunches or the energy i.e. stiffening the beam are all expected to improve luminosity. Unfortunately, increasing the number of bunches (and duty factor) produces multi-bunch instabilities and other problems when the total number of bunches exceeds the number of IR's. Thus, one seldom sees a linear increase in luminosity with n unless $\Delta\nu \ll \Delta\nu^*$. Decreasing either β_y^* or increasing the horizontal emittance ϵ_x reduces the beam-beam force but is difficult because this increases the sensitivity to transverse instabilities. Decreasing β_y^* also implies shorter bunches which increases the sensitivity to transverse-longitudinal couplings i.e. synchrotron resonances. Using wigglers in existing rings to increase ϵ_x with decreasing energy⁵ is now rather well established and relatively benign but the reverse is not true for this relies on tracking and simulation studies of nonconservative, nonintegrable systems.

Evidence from many rings has shown⁶ that $\Delta\nu^* \lesssim 0.05$ and that it is difficult to keep this matched in both directions with increasing beam currents. Nevertheless, this number can presumably be increased in a variety of ways e.g. by increasing damping by going to higher bend fields (and thus also increasing f) or by incorporating more wigglers. Although the observed magnitude of $\Delta\nu^*$ seems small, it is useful to compare it to the tune spread induced by ripple in the strong IR quads where typical tolerances are $10^{-4} < \delta k/k < 10^{-3}$ e.g.

$$\frac{\delta\nu_Q}{\frac{\delta k_Q}{k_Q}} = \frac{N_Q}{4\pi} \beta_Q(m) k_Q(m^{-1}) \simeq \begin{cases} 90 & \text{(PEP)} \\ 25 & \text{(SPEAR)} \end{cases}$$

where N_Q is the number of quads with strength k_Q or inverse focal length. Summing over all quad families in a ring gives numbers comparable to $\Delta\nu^*$. Furthermore, because the multipole expansion of the beam-beam interaction goes to high order and these multipoles can't be reduced by simply increasing the aperture as for quadrupoles it is clear that the linear description of the beam-beam interaction is not adequate. At the same time, it is not at all clear how to deal with such nonlinearities or even to simulate them in a self-consistent way. This ultimately involves the question of stochastic behavior in storage rings where even the most fundamental question of stability has not been proven. Furthermore, very little effort has gone into this and related questions such as multibunch instabilities.

⁵ J.M. Paterson, J.R. Rees and H. Wiedemann, PEP Note 125 (1975); W. Brunk, G. Fischer and J. Spencer, IEEE Nucl. Sci. **26** (1979) 3860.

⁶ See for example: H. Wiedemann, SLAC-PUB-2320, 1979.

I will not go into the many attempts to compensate or cancel $\Delta\nu$ except to mention the charge-neutralization scheme of the Orsay Group⁷ using 4 beams and double rings. It was hoped this approach would provide an improvement in \mathcal{L}_{max} of two-orders of magnitude but so far has not been made to work. The Stanford single-pass collider (SLC) represents the opposite extreme where it seeks to maximize $\Delta\nu^*$ with high bunch current and low-emittance to enhance luminosity through a pinch effect. The attitude we have taken is to avoid the beam-beam problem through conversion of the charged particles into photons. The limits in this case are presumably the maximum, single bunch currents which a linac can provide and a storage ring can store with good stability and emittance. This can be limited by many external effects before internal space-charge becomes important but again there is very little systematic information available on this question.

Systematic machine physics studies on PEP with a single beam that are relevant to these questions include bunch cross-section measurements versus all of the following: bunch current (N_b); bunch number (n_b) and distribution; both high and low $\beta_{x,y}^*$; ν_s , σ_z , σ_ϵ and V_{RF} ; and $\nu_{x,y}$. These should be done at a couple of energies e.g. a low (5 GeV), intermediate (10 GeV) and high energy (15-18 GeV). Any instabilities observed should be characterized by their threshold behavior (N_{th}) versus these parameters including possible differences between electrons and positrons.

4. Compton Characteristics and Applications

It was predicted⁸ and verified⁹ that Compton backscattering of polarized laser beams could produce quasi-monochromatic, polarized beams of high energy photons. Because this is a two-body process with the incident energies and angles proscribable within narrow limits, it follows that the energy of the outgoing photon (ω_2) depends only on its laboratory scattering angle relative to the incoming particle beam (θ_2) and the energies of both incident particle ($\epsilon_1 \equiv \gamma m_1$) and incident photon (ω_1):

—7 J.E. Augustin et al., VIIth Int'l. Conf. on High Energy Accelerators, Vol. 2 (1969) 113.

8 R.H. Milburn, Phys. Rev. Lett. **10** (1963) 75; F.A. Arutyunian, I.I. Goldman and V.A. Tumanian, Pisma ZHETF **45** (1963) 312.

9 J. Ballam et al., Phys. Rev. Lett. **23** (1969) 498.

$$\frac{\omega_2}{\omega_1} = \frac{1 - \beta \cos \theta_1}{1 - \beta \cos \theta_2 + \frac{\omega_1}{\epsilon_1}(1 - \cos \phi)};$$

$$\frac{\omega_2}{\omega_1} \simeq 4\gamma^2 \frac{[1 - (\theta/2)^2]}{1 + (\gamma\theta_2)^2 + 4\gamma\frac{\omega_1}{m_1}[1 - (\theta/2 + \theta_2/2)^2]} \simeq \frac{4\gamma^2}{1 + (\theta_2\gamma)^2 + 4\gamma(\frac{\omega_1}{m_1})}$$

$$\left(\frac{\omega_2}{\omega_1}\right)_{max} = \frac{4\gamma^2}{1 + 4\gamma(\omega_1/m_1)}; \quad x \equiv \left(\frac{\omega_2}{\epsilon_1}\right)_{max} = \frac{4\gamma(\omega_1/m_1)}{1 + 4\gamma(\omega_1/m_1)} \equiv \frac{z}{1+z}.$$

The variation in the energy of the outgoing photons varies primarily with θ_2 but only weakly with incident photon direction, θ . Maximum energy transfer occurs when both $\theta = \theta_2 = 0$. With lasers ($\omega_1 \approx 1eV$) the incident particle mass only becomes significant (10% level) for electrons at PEP and SLC energies of $\epsilon_1 \gtrsim m_1^2/(40\omega_1) \gtrsim 6 GeV$. With higher incident photon energies from undulators ($\omega_1 \approx 1 - 10^3 KeV$) the mass term becomes significant even for moderate proton energies ($\epsilon_1 \gtrsim 20 GeV$). Tables III (electrons) and IV (protons) give the peak photon energies produced from Compton conversion of quasimonochromatic photons produced by various processes ranging from lasers to coherent bremsstrahlung.

The energy spread of the photon beam $\delta (\equiv \delta\omega_2/\omega_{2max})$, for reasonably small incident particle or photon divergences (θ), can be written in terms of an effective collimation angle (θ_2^c) as:

$$\delta = \frac{\omega_{2max} - \omega_2(\theta_2^c)}{\omega_{2max}} = \frac{(\theta_c\gamma)^2}{1 + (\theta_c\gamma)^2 + 4\gamma(\frac{\omega_1}{m_1})}.$$

Compton scattering by free electrons is described by the Klein-Nishina formula (1929) and for moving electrons by Feenberg and Primakoff (1948). The cross section for $\theta = 0$ can be expressed in terms of the dimensionless variables x, z and $y \equiv 1 - x$:

$$\frac{d\sigma^C}{dx} = \frac{\sigma_o}{z} \left[y + \frac{1}{y} - \frac{4x}{zy} + \frac{4x^2}{z^2y^2} \right] \xrightarrow{x \rightarrow 1} \sigma_o$$

where $\sigma_o \equiv 2\pi r_e^2 = \frac{1}{2}$ barn with the total C-M energy $s/m_e^2 = 1 + z$. Figure 2 show $d\sigma^C/dx$ for the electrons of Table III and Fig. 3 shows $d\sigma^C/dx$ for the

protons of Table IV. The total Compton cross section, depending only on s , is:

$$\sigma^C = \frac{\sigma_0}{z} \left[\left(1 - \frac{4}{z} - \frac{8}{z^2}\right) \ln(z+1) + \frac{8}{z} + \frac{1}{2} \left(1 - \frac{1}{(z+1)^2}\right) \right] \xrightarrow{z \rightarrow 0} \frac{4}{3} \sigma_0.$$

Tables V and VI give the total and peak cross sections for electrons. The total cross section approaches a maximum which is just the Thomson cross section ($\frac{2}{3}$ barn) for lasers on SPEAR beams. Increasing ω_1 or ϵ_1 , increases ω_2 and eventually its monochromaticity but decreases the production rate. Assuming one can control the monochromaticity of ω_1 and the angular spread of the electrons, it follows that control of the energy spread of ω_2 is controlled by the angular acceptance.

Fortunately, the scattering cross section is very strongly peaked in the forward direction where the momentum transfer falls quadratically with θ_2 so the photons are naturally collimated. Photons at $\theta_2 = 0$ maximize ω_2 while those at $\theta_2 = \pi$ are unchanged. The differential cross section is

$$\frac{d\sigma^C}{d\Omega_2} = \frac{\sigma_0}{4\pi\gamma^2} \left(\frac{\omega_2}{\omega_1}\right)^2 \left[\left(\frac{1}{u} - \frac{1}{z}\right)^2 - \left(\frac{1}{u} - \frac{1}{z}\right) + \frac{1}{4} \left(\frac{u}{z} + \frac{z}{u}\right) \right] \xrightarrow{u \rightarrow 1} \frac{\sigma_0}{4\pi} \left(\frac{\epsilon_1}{\omega_1}\right)$$

which is again expressed in terms of normalized four-products $u = \frac{2}{m_e^2} (p_1 \cdot k_2)$ and $z = \frac{2}{m_e^2} (p_1 \cdot k_1) \rightarrow 4\gamma(\omega_1/m_e)$. Plots corresponding to the above examples are shown in Fig. 4. At the collision point a parallel, low-emittance electron beam is preferred for many such applications i.e. a high-tune, mini-maxi configuration for PEP seems preferable. Tradeoffs between energy, intensity and background determine the optimum values of (ω_1, ϵ_1) .

The backgrounds require detailed calculations of a number of processes, just as for electrons, but the dominant loss mechanism of Bhabha scattering is not present. Furthermore, low-beta insertions produce significant amounts of "high-energy" synchrotron radiation that is literally focused onto the counter-rotating beam. With photon beams, it is probably the conversion electrons that are of most concern but they are predominantly scattered into the very forward direction as shown in Fig. 5. These results imply that $\omega_1 \lesssim 1$ KeV should not produce background from the scattered electrons, for well aligned beams, because of their very small divergence or energy. The beauty of the SLC beam for this application is that it is well matched to current laser capabilities and PEP energies.

Applications based on these equations can be defined based on whether there is a relative energy gain or loss by ω_1 as follows:

$\theta_1 = 0^\circ$	$\theta_2 = 0^\circ$	$\omega_2/\omega_1 = 1$	Coherent Bunching
	$\theta_2 = 90^\circ$	$\omega_2/\omega_1 = 1/2\gamma^2$	Inverse Undulator/Accelerator
$\theta_1 = 90^\circ$	$\theta_2 = 0^\circ$	$\omega_2/\omega_1 = 2\gamma^2$	Undulator Condition
	$\theta_2 = 90^\circ$	$\omega_2/\omega_1 = 1$	Mirror/Transmission Detector
$\theta_1 = 180^\circ$	$\theta_2 = 0^\circ$	$\omega_2/\omega_1 = 4\gamma^2$	Optimal photon acceleration
	$\theta_2 = 90^\circ$	$\omega_2/\omega_1 = 2$	Energy doubling

Polarization effects have probably received more attention because of the relative simplicity of asymmetry measurements. The scattering of circularly polarized light by e^\pm can be used to measure polarization¹⁰ of the e^\pm and also be used to induce it. A low-energy, polarized electron beam can be used in a similar way to the photon beam to measure the polarization of a stored electron beam¹¹ or to polarize photons via Compton scattering. Compton scattering of synchrotron radiation by stored beams can be a serious cause of lifetime loss as well as detector noise so that most rings including SLC take careful precautions to guard against it through detailed simulations of additional elements such as masks and low field bends. In this sense, the addition of wigglers and chicanes in this region is not at all atypical. It is interesting that a variety of usable setups have been employed at many rings for diagnostic purposes and presumably could be used in many other ways – just like the storage rings themselves.

5. Photons, Electrons or Both?

Another reason for converting electrons to photons is based on the equivalent photon approximation of Weizsacker and Williams or the fact that the spectral distribution of the electron's field is equivalent to a field of virtual photons with the same energy distribution. In this sense, the electron has been called photon-like (albeit virtual etc.) and so one might reasonably ask under what conditions the effective luminosity can be improved by using real photons. Using only a storage ring, this may seem absurd because it would destroy the lifetime but this isn't necessarily so as we show below. The equivalent number of virtual photons

¹⁰ C.Y. Prescott, SLAC TN-73-1 (1973).

¹¹ D. Buchholz, G. Manning and C. Prescott, PEP Note 173 (1976).

per electron^{12 13} or $e\gamma$ vertex in the range dx of scaled photon energy ($x = \frac{\omega_2}{\epsilon_1}$) is:

$$\frac{dN_\gamma(\epsilon_1, x)}{dx} \simeq \left(\frac{\alpha}{\pi}\right) \ln\left(\frac{2\epsilon_1}{m_e}\right) \left[\frac{1 + (1-x)^2}{x}\right].$$

This expression is based on integrating over the full angular range of the electrons whose energy $\gamma_1 \gg (1-x)/2x$. The number in the interval from full energy to $x\epsilon_1$ is:

$$\int_1^x dx \frac{dN_\gamma}{dx} = \left(\frac{2\alpha}{\pi}\right) \ln\left(\frac{2\epsilon_1}{m_e}\right) G(x)$$

where $G(x) = x + \frac{1}{2}(1-x^2) - \ln x$. For $\epsilon_1 \lesssim 10$ GeV and $x = 0.9$, in the deep inelastic region, there are less than 5×10^{-3} photons per electron and for $x \geq 0.1$ there are still less than $0.09 \gamma's/e$. Because this expression overestimates the number of photons theoretically and since the experiments have both limited angular acceptance and efficiency it provides a very conservative upper bound on the relative gain to be expected from using real photons.

The reaction rate (and ideally the counting rate) for a process such as shown in Fig. 1f or 1g, when using real photons, can be obtained from

$$\frac{dN_X}{dt} = \mathcal{L}_{\gamma\gamma} \sigma_{\gamma\gamma \rightarrow X}(s_{\gamma\gamma}) \equiv \frac{N_{\gamma_1} N_{\gamma_2}}{4\pi\sigma_x^* \sigma_y^*} f \sigma_{\gamma\gamma \rightarrow X},$$

where $s_{\gamma\gamma} = 4\omega_1\omega_2$. The corresponding rate, with one real photon and one electron in the incident channel will be

$$\frac{dN_X}{dt} = \mathcal{L}_{e\gamma} \sigma_{e\gamma \rightarrow X}(s_{e\gamma} = 4\omega_1\epsilon_1) \equiv \int dz \frac{dL_{e\gamma}}{dz} \sigma_{\gamma\gamma \rightarrow X}(z)$$

with $\sigma_{\gamma\gamma}$ the spectral cross section for head-on collisions and $z = s_{\gamma\gamma}/4\omega_1\epsilon_1 \approx \omega_2/\epsilon_1 = x$. The equivalent photon, differential luminosity function is defined as:

$$\frac{dL_{e\gamma}}{dz} = \mathcal{L}_{e\gamma} \left(\frac{2\alpha}{\pi}\right) \ln\left(\frac{2\epsilon_1}{m_e}\right) \frac{1}{z} G(z).$$

Finally, the same reaction channel in the conventional, two-photon reaction with

¹² F.E. Low, Phys. Rev. **120** (1960) 582.

¹³ S.J. Brodsky, T. Kinoshita and H. Terazawa, Phys. Rev. D **4** (1971) 1532.

two incident electrons is:

$$\frac{dN_X}{dt} = \mathcal{L}_{ee} \sigma_{ee \rightarrow X}(s_{ee} = 4\epsilon_1^2) \equiv \int dz \frac{dL_{ee}}{dz} \sigma_{\gamma\gamma \rightarrow X}(z)$$

where $z = s_{\gamma\gamma}/4\epsilon_1^2 \simeq \omega_1\omega_2/\epsilon_1^2 = x_1x_2$ for nearly real photons and an equivalent photon luminosity function:

$$\frac{dL_{ee}}{dz} = \mathcal{L}_{ee} \left[\left(\frac{2\alpha}{\pi} \right) \ln \left(\frac{2\epsilon_1}{m_e} \right) \right]^2 \frac{1}{z} F(z).$$

with $F(z) = -\frac{1}{2}(2+z)^2 \ln z - (1-z)(3+z)$ the same function derived by Low¹².

The effective luminosity decreases by successive powers of $(\frac{2\alpha}{\pi}) \ln(\frac{2\epsilon}{m_e}) \sim 1/20$ for $\epsilon \sim 10$ GeV for a perfect, 4π detector with *neither* noise nor channel competition from other diagrams such as Bhabha scattering. At higher momentum transfers, the rate falls drastically from the G and F factors while at lower momentum transfers, angular cutoffs and momentum thresholds become significant e.g. Low's original proposal for the pion where $X \equiv \pi^0$ still hasn't been done accurately even though this is quite important.¹⁴ Furthermore, where higher mass particles are involved, such as η_b , $A2_b$, ... etc., it appears there is very little possibility of observing these in the conventional 2-photon reaction – at least at PEP unless one pushes the energy considerably higher than is likely.

6. Example I: Linac Photon Beam with PEP Positron Beam

One way to increase C-M energy with existing storage rings is to collide them with upgraded linac beams.¹⁵ At SLAC, the SLC upgrade of the linac provides an ideal example of such a scheme.¹⁶ This was revived to search for the top quark via annihilation to $q_t \bar{q}_t$ at higher energies before the “truth” of the matter put it above the ceiling of PEP, PETRA or TRISTAN. Perhaps the most important point to be made here is that this again illustrates the dominant importance of the critical current because this approach is again limited below optimum luminosity (\mathcal{L}_{max}) by the critical current of the linac bunch N_L^* .¹⁶ An alternative is to convert the linac beam into photons and collide these with the PEP stored beam. This provides a simple example of the basic ideas here.

¹⁴ S.J. Brodsky and G. P. Lepage, Phys. Rev. **D24** (1981) 1808; S. J. Brodsky, SLAC-PUB-3440 (1984) and SLAC-PUB-3547 (1985).

¹⁵ P.L. Csonka and J.R. Rees, NIM **96** (1971) 149.

¹⁶ J.R. Rees and H. Wiedemann, PEP Note-324 (1979) and R. Stroynowski, SLAC PUB-2451 (1979).

The benchmark, invariant emittance for SLC is, without the usual factor of π , $\epsilon_L \equiv \gamma\sigma\sigma' = 3 \times 10^{-5}$ rad·m for $N_L = 5 \times 10^{10}$. The transverse emittance decreases with increasing energy from the linac while it increases proportional to $(E(\text{GeV})/15)^2$ in PEP. Assuming a fully coupled beam in PEP ($K = 1$) it is possible, according to Rees and Wiedemann¹⁶, to obtain an emittance $\epsilon_P = 1.2 \times 10^{-8}$ rad·m at 15 GeV. This reduces to $\epsilon_P = 5.3 \times 10^{-9}$ rad·m at 10 GeV compared to $\epsilon_L = 8.5 \times 10^{-10}$ at $\epsilon_1 = 30$ GeV i.e. $\epsilon_P/\epsilon_L \sim 6$. Assuming we can nearly convert the linac electrons into quasi-monochromatic photons using a laser or PEP undulator then gives:

$$\mathcal{L}_{e\gamma} = \frac{N_P N_L}{4\pi\beta^*\epsilon_P} f_L = \frac{7 \times 10^{30}}{\beta^*(\text{cm})} \left[\frac{I_P}{100\text{mA}} \right] \left[\frac{10}{E(\text{GeV})} \right]^2 \text{cm}^{-2}\text{s}^{-1},$$

for a linac rep rate of $f_L = 180/\text{s}$. A low- β^* of $\lesssim 1$ cm should be possible in a way that doesn't increase emittance due to high-order aberrations just as for SLC.¹⁷ A 30 GeV beam with $\omega_1 \sim 1$ eV photons gives $\omega_2 \sim 10$ GeV photons i.e. $\sqrt{s} = E_{cm} \sim 20$ GeV – the same as for conventional 10 GeV colliding beams.

If $\mathcal{L}_{ee} \sim 2 \times 10^{31}$ at 15 GeV and scales as E^2 , then the effective $\mathcal{L}_{e\gamma}$ achieved in \mathcal{L}_{ee} must necessarily be less than that for real photons while deep inelastic contributions will be down by several orders of magnitude. Although the photon emittance (ϵ_γ) increases as the square of the distance from the $e\gamma$ interaction point, the variable energy of the linac beam and its lower emittance allow ϵ_γ to be matched to ϵ_P with natural energy collimation. The number of incident laser photons is just $N_\gamma^L = A_L/\sigma_c \sim 10^{19}$ at $f_L = 180/\text{s}$ in a pulse of length 10 ps.

7. Example II: Photon-Photon Scattering and Reactions

One can do high energy $\gamma\text{-}\gamma$ scattering in several possible ways e.g. similar to the $e\text{-}\gamma$ method above except that part ($\sim 1\%$) of the stored beam is now also converted into high energy photons (and replenished by continuous reinjection) or simply use both SLC beams in a variant of the $\gamma\text{-}\gamma$ scheme for SLC². Another possibility is to use two, high current e^\pm beams in PEP which are separated at the IR and used instead to produce two primary, high intensity, low energy photon beams as in the previous example to study diagrams g and h from very low energies upwards i.e. do a $\gamma\text{-}\gamma$ excitation function or energy scan. Although this was calculated as early as 1936 by Euler and Heisenberg, I believe there are still

¹⁷ J.E. Spencer, SLAC-CN-264 (1984).

virtually no experiments on it. For $\omega_1 = \omega_2 \equiv \omega \ll m$, the differential, elastic scattering cross section is

$$\frac{d\sigma}{d\Omega} = \frac{\alpha^4}{\pi} \frac{A}{m^2} \left(\frac{\omega}{m}\right)^6 (3 + \cos^2 \theta)$$

where $A = 139/(90)^2$ and the total cross section is

$$\sigma = \frac{\alpha^4}{\pi} A \left(\frac{56}{5}\right) \frac{1}{m^2} \left(\frac{\omega}{m}\right)^6.$$

From Table I the cross section falls with photon energy for $\omega \gg m$ so it presumably peaks near $\omega \sim m$ with a cross section on the order of $1 \mu\text{b}$. With a 1-2% RF capture bucket and stored currents of 100 mA near 10 GeV one could expect primary photon intensities

$$\frac{E_e}{100\omega} N_e \approx 5 \times 10^{20}$$

for $\omega \approx 1 \text{ eV}$ i.e. more than enough to do this experiment and even the previous one for anything like the expected bunch cross sections over a large energy range.

8. Example III: Internal Targets in PEP

Although fixed-target experiments were discussed some twenty-five years ago in the original storage ring proposal,¹⁹ little or no work of this kind has been done even though there are many interesting and significant QCD studies²⁰ possible. We can write the equivalent luminosity in terms of the target thickness, n_t , in $\#/\text{cm}^2$ as

$$\mathcal{L} = N_b \left(\frac{N_t}{A}\right) f = \left(\frac{I_b}{e}\right) N_A \left(\frac{\rho x}{A}\right) = \left[\frac{I_b}{100 \text{ mA}}\right] \times \left[\frac{n_t}{10^{15}/\text{cm}^2}\right] \times 6.2 \times 10^{32} \text{ cm}^{-2} \text{ s}^{-1}$$

where N_A is Avogadro's number and A is the gram-molecular weight of the target. Targets on the order of $n_t \sim 10^{15}/\text{cm}^2$ are very thin compared to typical high resolution spectrometer targets of 1-100 mg/cm^2 such as used at Bates, LAMPF

¹⁹ Barber, O'Neill, Panofsky and Richter, Proposal to U.S.A.E.C. dated May, 1958.

²⁰ S.J. Brodsky, private communication.

or SLAC but appear *ideal* for optically pumped, *polarized* targets²¹ for a large range of atomic numbers including H¹, D² and He³ i.e. the 3, 6 and 9 quark systems. The primary sources of noise in the target (e.g. due to bremsstrahlung) which depend on n_t^2 will generally be negligible while asymmetry measurements require good angular resolution but need not be limited by the small solid angle of spectrometers. Because \mathcal{L} does not depend on the beam cross-sectional area, one can consider operating in a maxi- β configuration with small angular spreads at the target *and* very high currents when not simultaneously colliding in other IR's. Table II gives the expected capabilities at SLAC using either SPEAR or PEP in single-beam or colliding modes.

Figure 6 from the PEP handbook shows the expected lifetimes due to various sources of loss in PEP. While this implies the importance of three different processes over the range of energies of interest, the most important one for our purposes is atomic bremsstrahlung since we assume the Touschek effect will only be important near the IR's and that the particle density can easily be varied by the required factor of two or so. This same factor of two might also be obtainable by manipulating $(\beta_{min}^*, \beta_{max}^*)$ in a mini-maxi beta scheme. This is clearly not a problem but bremsstrahlung from "residual-gas" is – because the differential probability for radiation loss is roughly constant up to the full electron energy for the electron energies of interest here. Integrating Rossi's expression²² for the differential radiation probability per unit radiation length gives:

$$\int_{(\frac{\delta\gamma}{\gamma})_{RF}}^1 \Psi_{rad}(x) dx = \left[\frac{4}{3} \ln\left(\frac{\gamma}{\delta\gamma}\right)_{RF} - \frac{5}{6} \right]$$

where x is the fractional photon energy, ω/ϵ . The fractional particle loss is then

$$\frac{dN_b}{N_b} = - \left[\right] \frac{\rho}{X_o} dx \longrightarrow \frac{1}{\tau} = \left[\right] \frac{c\rho}{X_o}$$

assuming a simple target uniformly distributed around the ring like residual gas. Here $1/X_o \equiv N_A \sigma_{rad}/A$ with σ_{rad} the total bremsstrahlung cross section per

21 R. J. Holt, private communication

22 Rossi, B., **High Energy Particles**, Prentice Hall, Inc. (1952).

nucleus or atom and x is the lineal thickness. In terms of both ring and target components, the expression is

$$\frac{1}{\tau} = [] \left[\sum_i \frac{c\rho_i^{STP}}{X_{oi}} \left(\frac{P_i}{760}\right) + \sum_j \frac{c\rho_j^{STP}}{X_{oj}} \left(\frac{l_t}{l_R}\right) \left(\frac{P_j}{760}\right) \left(\frac{273}{T_j}\right) \right]$$

where l_t/l_R is the ratio of target length to ring circumference. Including both the atomic bremsstrahlung cross section for electrons and nucleus so that $\sigma_{rad}^i = 4\alpha Z_i(Z_i + 1)r_e^2[\ln 183/Z_i^{1/3} + \frac{1}{18}]$ but ignoring all but one target component (i.e. considering only the partial lifetime due to the target) in an otherwise perfect vacuum gives:

$$\frac{T_o}{\tau_t} \simeq [] 4\sigma_o Z(Z + 1) \ln(183/Z^{1/3}) \left[\frac{N_A}{A} \rho^{STP} l_t \left(\frac{P}{760}\right) \left(\frac{273}{T}\right) \right].$$

The last factor in brackets is just the target thickness n_t (#/unit area), $\sigma_o \equiv \alpha r_e^2$ and T_o is the revolution time around the ring (see Table II). For hydrogen, $\rho_{H_2}^{STP} = 0.090 \text{ kG/m}^3$ so for $l_t = 10 \text{ cm}$

$$n_t = \frac{2N_A}{A_{H_2}} \rho_{H_2}^{STP} l_t \left(\frac{P_t}{760}\right) = 5.38 \times 10^{20} \left(\frac{P_t}{760}\right) [\text{atoms/cm}^2].$$

For $n_t = 10^{14}/\text{cm}^2$, this implies $P_t = 1.4 \times 10^{-4}$ Torr or a required differential pumping rate of $\sim 10^{-5}$ Torr at room temperature which is reasonable. One wants this differential rate to roughly correspond to the l_t/l_R factor ($\simeq 4.5 \times 10^{-5}$ in PEP) since the two main, residual gas components observed with mass analyzers are hydrogen and carbon monoxide.

Because the RF capture bucket width can be $\delta\epsilon_e/\epsilon_e \gtrsim \pm 1\%$ in both SPEAR and PEP, the corresponding partial lifetime for a $10^{14}/\text{cm}^2$, hydrogen target is:

$$\frac{\tau_t^H}{T_o} \simeq (5.31 \times 4 \times 0.58 \text{ mb} \times 10.42 \times 10^{14})^{-1} = 7.8 \times 10^{10} \begin{cases} 159 \text{ hrs} & (\text{PEP}) \\ 16.9 \text{ hrs} & (\text{SPEAR}) \end{cases}$$

This indicates these experiments can be done on both SPEAR and PEP²³ without requiring dedicated operation with $\mathcal{L} \gtrsim 10^{33} \text{ cm}^{-2}\text{s}^{-1}$ using state-of-the-art

23 Albert Hofmann has found essentially the same result independently.

polarized gas targets! This is independent of beam energy and valid for all energies of current interest ($\epsilon \gtrsim 1.5 \text{ GeV}$) as well as elements with $\alpha Z \ll 1$. PEP, with its large radius and large energy range, would seem to be an ideal system for these experiments especially when multibunch operation with higher duty factor and current is developed. These operating conditions are ideally matched to simultaneous synchrotron radiation operation.

9. A Few Conclusions(and Possibilities)

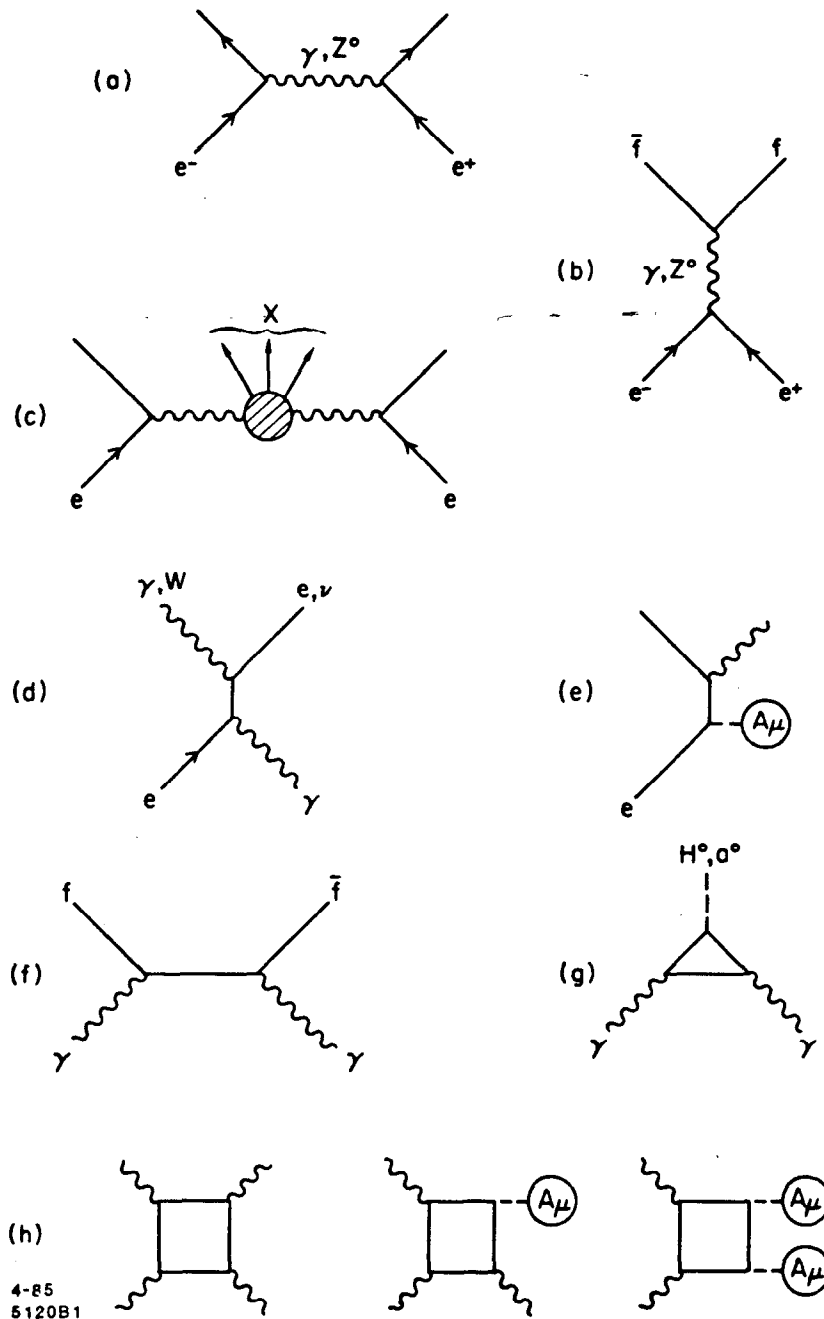
Assuming that either one or both injection IR's will be available at PEP, there are a remarkable number of possibilities available that can be arranged into an interesting, long-range program with well defined stages. Current plans for a mini-beta upgrade should allow a variable mini-maxi scheme in which at least one injection IR can run with variable high-beta during high energy physics operation since it is possible to do good, high-luminosity $\vec{e} + \vec{A}$ experiments in a noninterfering mode. Variable density targets, in conjunction with wigglers could improve low-energy, colliding beam operation by providing independent control over longitudinal and transverse phase space. Implementing longitudinal polarization with the new, efficient, tensor polarized gas targets could then provide an absolutely unique facility for nuclear QCD studies from 4-18(25) GeV. Multibunch operation in a dedicated mode of operation could provide duty factors of 10% or so with very high currents at the lower energies.

Implementing a high energy photon facility would augment the internal target program as well as the high energy physics studies since one wants to use such beams near their source even though good external photon beams will naturally arise. There are many interesting research and development projects here such as the study of high current, high density bunches; development of highly segmented, fast, efficient photon detectors and the development of long, combined function undulators²⁴ to name a few. An injection IR is clearly preferred for this work which would allow high luminosity $\vec{e} + \vec{\gamma}$ and $\vec{\gamma} + \vec{A}$ studies as well as $\vec{\gamma} + \vec{\gamma}$ over a large energy range. Photoproduction of hyper or other nuclear systems based on strange, charmed or bottom quarks might well prove to be the best way to study the quarks i.e. their structure and interactions.

10. Acknowledgements

— The author would like to thank many people for their interest and suggestions but especially Stan Brodsky, Fred Erne, Albert Hofmann and Bill Spence.

²⁴ J.E. Spencer, SLAC-PUB-3646, April 1985.



4-85
5120B1

Fig. 1: Low order diagrams in the standard model for: (a,b) elastic, electro-weak scattering; (b) electron-positron annihilation into elementary fermions $f = e, \mu, \tau \dots q_u, q_d, q_s \dots \nu_e, \nu_\mu, \nu_\tau \dots$ as well as elementary bosons (W^\pm, Z^0, H^0, H^\pm ?); (c) two-boson, electro-weak production; (d) Compton scattering or conversion ($\gamma \rightarrow W^\pm$); (e) potential bremsstrahlung; (f) two-photon annihilation to fermions; (g) two-photon annihilation to bosons; and (h) photon-photon scattering, inverse photon bremsstrahlung (harmonic production) and Delbrück scattering.

Table I: Scaling estimates of partial cross sections ($s/m_f^2 \gg 1$) for the processes of Fig. 1 with $e_f \equiv$ fermion charge in units of e . Cross sections are in the laboratory system for unpolarized photons. Angles are specified between incident and outgoing momenta and expressions should be valid for most experimental cuts and especially for loss of beam lifetime while colliding.

a)	$e^\pm \rightarrow e^\pm$	$\frac{d\sigma^{Bh}}{d\Omega} = \frac{\alpha^2}{4s} \left(\frac{3+\cos^2\theta}{1-\cos\theta} \right)^2$	$\sigma^{Bh} = \frac{16\pi\alpha^2}{s} \left[\frac{1}{4\sin^2 x} + \ln(\sin x) + \frac{1}{3} \right]_{x=\frac{\theta_{min}}{2}}$
b)	$e^\pm \rightarrow f\bar{f}$	$\frac{d\sigma^A}{d\Omega} = \frac{\alpha^2}{4s} (1 + \cos^2\theta) e_f^2$	$\sigma^A = \frac{4\pi\alpha^2}{3s} e_f^2$
c)	$e^\pm \rightarrow e^\pm X$		$\sigma^X = \frac{\alpha^4}{\pi m_e^2} \left(\frac{m_e}{m_f} \right)^2 e_f^4 \ln^2(s/m_e^2) \ln(s/m_f^2)$
d)	$e\gamma \rightarrow e\gamma$	(see text)	$\sigma^C = \frac{2\pi\alpha^2}{s} [\ln s/m_e^2 + 1/2]$
e)	$eA \rightarrow e\gamma$	(see text)	$\sigma^{SB} = 2Z^2 \frac{\alpha^3}{m_e^2} [\ln(s/m_e^2) - \frac{1}{3}]$
f)	$2\gamma \rightarrow 2f$	$\frac{d\sigma}{d\Omega} = \frac{\alpha^2}{s} \left[\frac{1+\cos^2\theta}{(4m_f^2/s + \sin^2\theta)} \right] e_f^4$	$\sigma = \frac{2\pi\alpha^2}{s} [\ln(s/m_f^2) - 1] e_f^4$
h)	$2\gamma \rightarrow 2\gamma$ $2\gamma \rightarrow 1\gamma$ $1\gamma \rightarrow 1\gamma$		$\sigma^{2\gamma} = \frac{4\pi\alpha^4}{s} e_f^4 \ln(s/m_f^2)$ $\sigma \propto \alpha Z^2 \sigma^{2\gamma}$ $\sigma \propto \alpha^2 Z^4 \sigma^{2\gamma}$

Table II: Some characteristic parameters for the SPEAR and PEP storage rings. Invariant emittance for an SLC bunch of 5×10^{10} is $\epsilon \equiv \gamma\sigma^2/\beta = 3 \times 10^{-5}$ m-r.

Energy(GeV)	2 SPEAR	5 PEP	10 PEP	15 PEP	
Damping Time, $\tau_{x,y}$	28.3	220	27.5	8.2	msec
Coupling, $K \equiv \epsilon_y/\epsilon_x$	6.3	6.3	7.6	7.6	%
Beam Current, I_e^{Max}	100	30(?)	100(?)	100	mA
Beam Current, I_t^{Col}	25	20	33	50	mA
Emittance, $\epsilon_x \equiv \sigma_x^2/\beta_x$	0.195	0.0138	0.055	0.124	mm-mr
Emittance, $\epsilon_y \equiv \sigma_y^2/\beta_y$	12.2	0.866	4.19	9.43	μ m-mr
Energy Spread, σ_E/E	0.024	0.033	0.067	0.10	%
Revolution Time, T_o	0.78	7.34	7.34	7.34	μ sec
IR Beta, β_x^*	0.9/20	3.0/15	3.0/15	3.0/15	m
IR Beta, β_y^*	0.03/35	0.12/0.6	0.12/0.6	0.12/0.6	m
IR Size, σ_x^*	0.42/1.97	0.20/0.45	0.41/0.91	0.61/1.36	mm
IR Size, σ_y^*	.019/0.65	.010/.023	.022/.050	.034/.075	mm
Divergence, $\sigma_{x'}$.465/.099	.068/.030	.136/.061	.203/.091	mr
Divergence, $\sigma_{y'}$.638/.019	.085/.038	.187/.084	.280/.125	mr

Table III: $(\omega_2/\epsilon_1)_{max}$ for various incident photon energies (ω_1) and incident electron energies (ϵ_1) for Compton scattering.

$\epsilon_1(\text{GeV}) =$	2	10	50	100	
ω_1	(SPEAR)	(PEP)	(SLC)	(LEP)	
1 eV	0.030	0.133	0.434	0.605	Lasers/FEL's
10 eV	0.235	0.605	0.885	0.939	
1 KeV	0.968	0.994	0.999	0.999	Wigglers
					Channeling
1 MeV	1.000	1.000	1.000	1.000	Coh. Brem.

Table IV: Values of $(\omega_2/\epsilon_1)_{max}$ for various incident photon energies (ω_1) and incident proton energies (ϵ_1).

$\epsilon_1(\text{GeV}) =$	50	500	1000	20×10^3
ω_1		(CERN/FNL)	(Tevatron)	(SSC)
1 eV	0.23×10^{-6}	0.23×10^{-5}	0.45×10^{-5}	0.91×10^{-4}
10 eV	0.23×10^{-5}	0.23×10^{-4}	0.45×10^{-4}	0.91×10^{-3}
1 KeV	0.23×10^{-3}	0.23×10^{-2}	0.45×10^{-2}	0.083
1 MeV	0.185	0.694	0.820	0.989

Table V: The total Compton cross sections σ_c (mb) corresponding to Table I.

$\epsilon_1(\text{GeV}) =$	2	10	50	100
ω_1	(SPEAR)	(PEP)	(SLC)	(LEP)
1 eV	646	580	409	319
10 eV	520	319	148	97
1 KeV	61	18	4.6	2.5
1 MeV	0.176	0.041	0.009	0.005

Table VI: Values of $(1/\sigma_0)(d\sigma_c/dx)_{max}$ for Table I. This differential cross section always occurs at $(\omega_2/\epsilon_1)_{max}$. $\sigma_0 \equiv 2\pi r_0^2 = 0.499$ barns.

$\epsilon_1(\text{GeV}) =$	2	10	50	100
ω_1	(SPEAR)	(PEP)	(SLC)	(LEP)
1 eV	65.3	13.2	3.05	1.91
10 eV	6.76	1.91	1.15	1.07
1 KeV	1.03	1.01	1.00	1.00
1 MeV	1.00	1.00	1.00	1.00

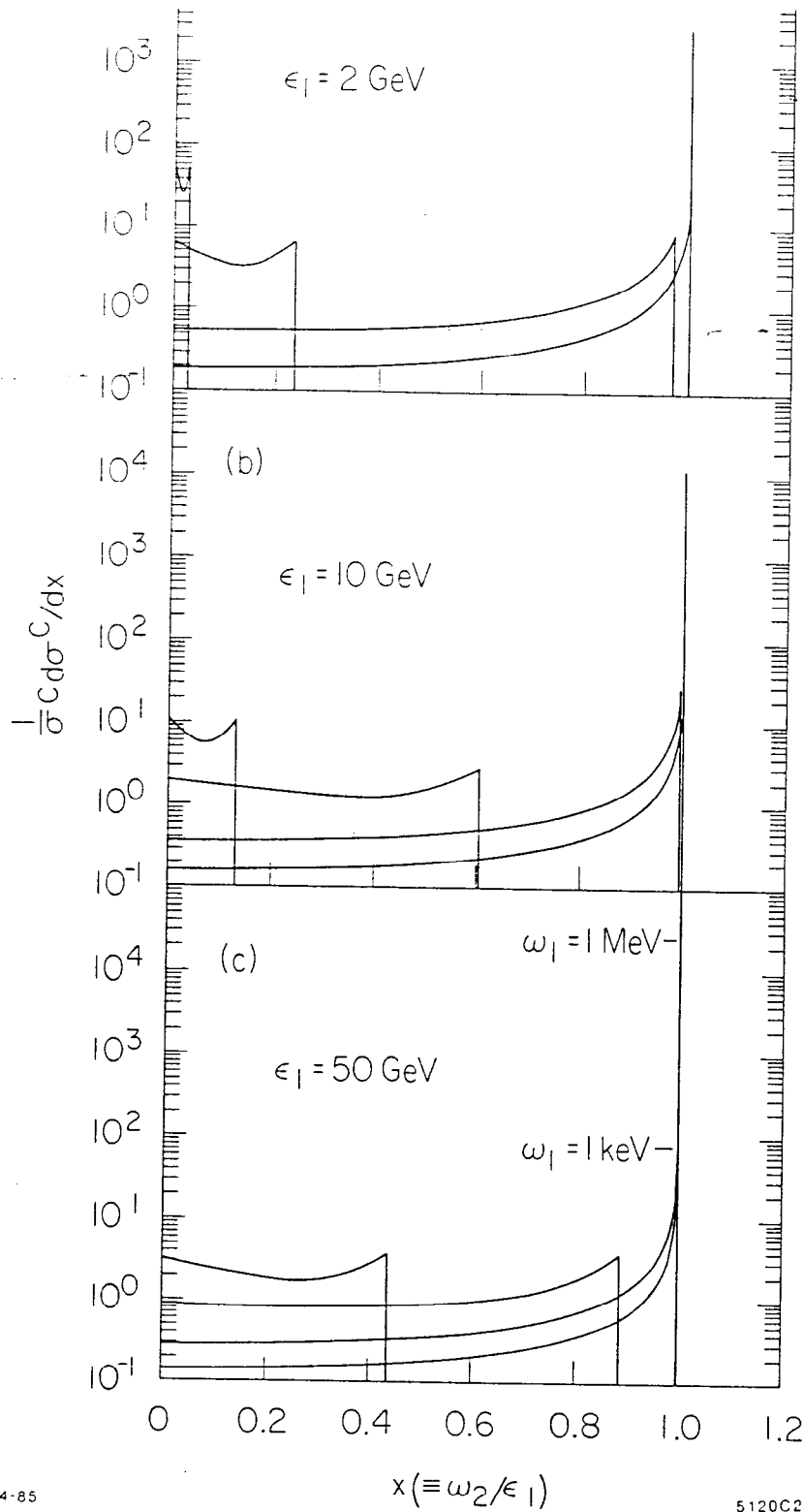
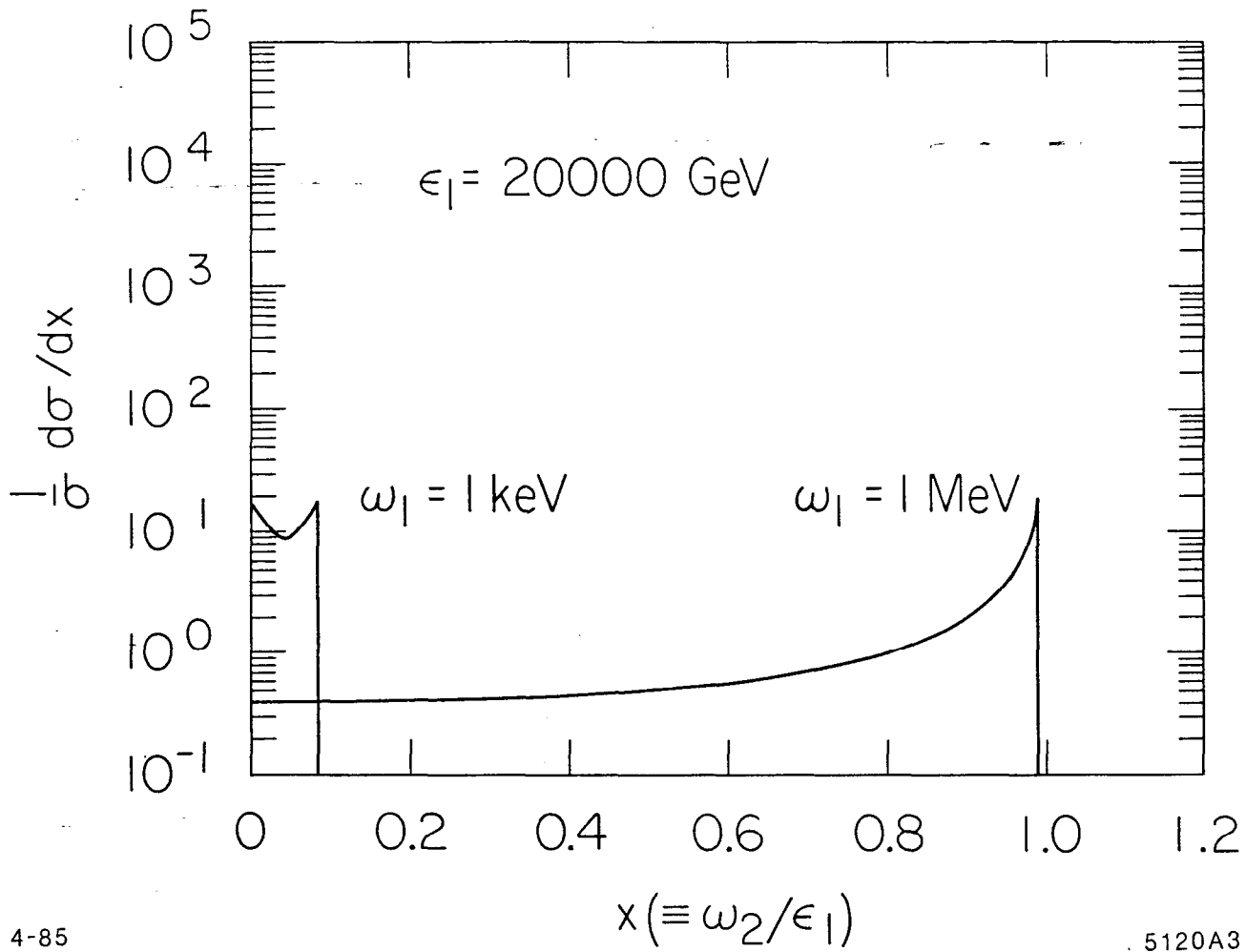


Fig. 2: Spectral cross sections for Compton scattering of $\omega_1 = 1, 10, 10^3, 10^6 \text{ eV}$ photons on SPEAR, PEP and SLC electrons. See also Tables 3,5 and 6.



4-85

5120A3

Fig. 3: Spectral cross sections for Compton scattering of $\omega_1 = 1, 10, 10^3, 10^6 \text{ eV}$ photons on SSC protons. See also Table 4.

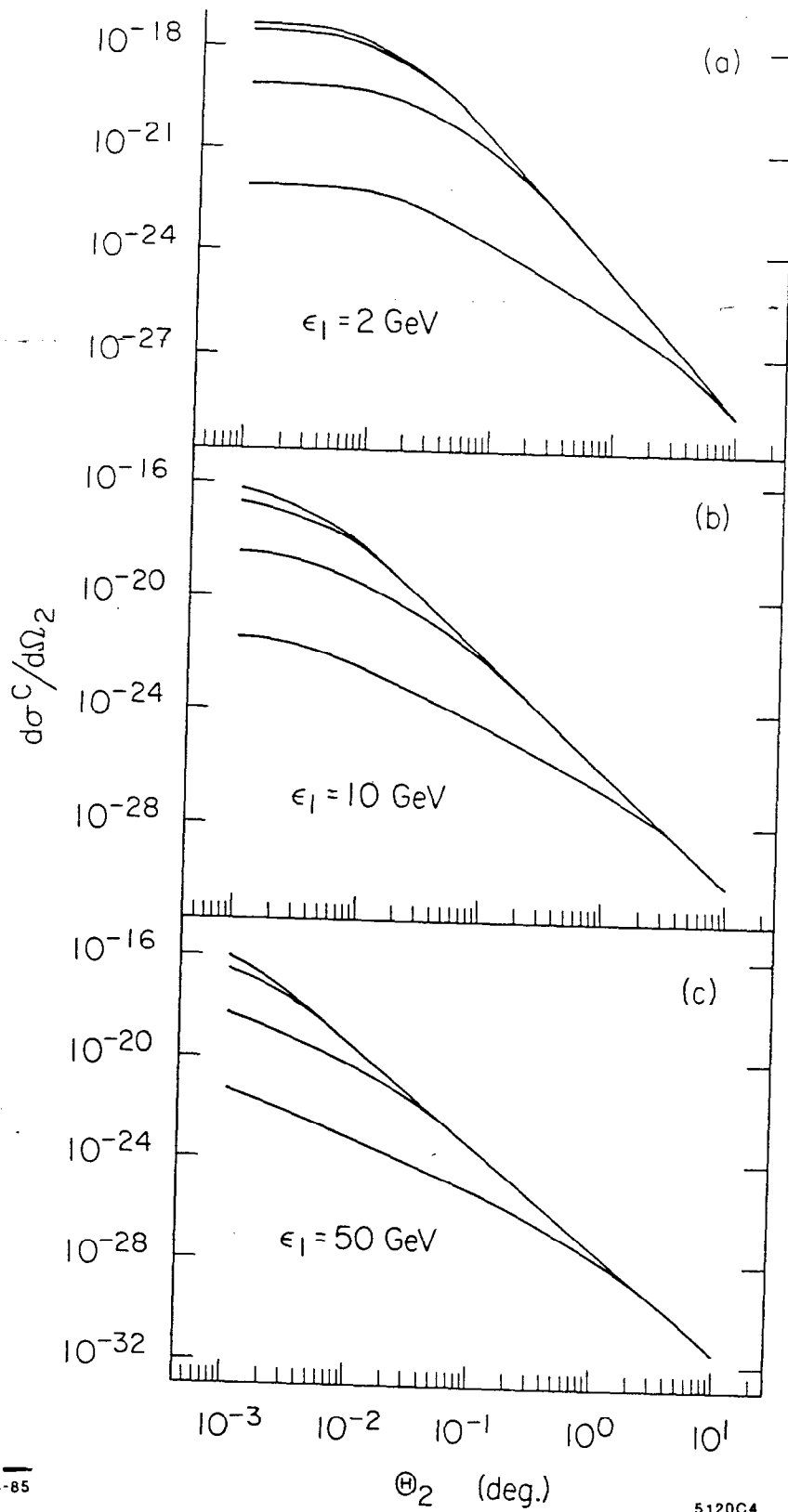


Fig. 4: Photon differential scattering cross sections corresponding to Figure 2.

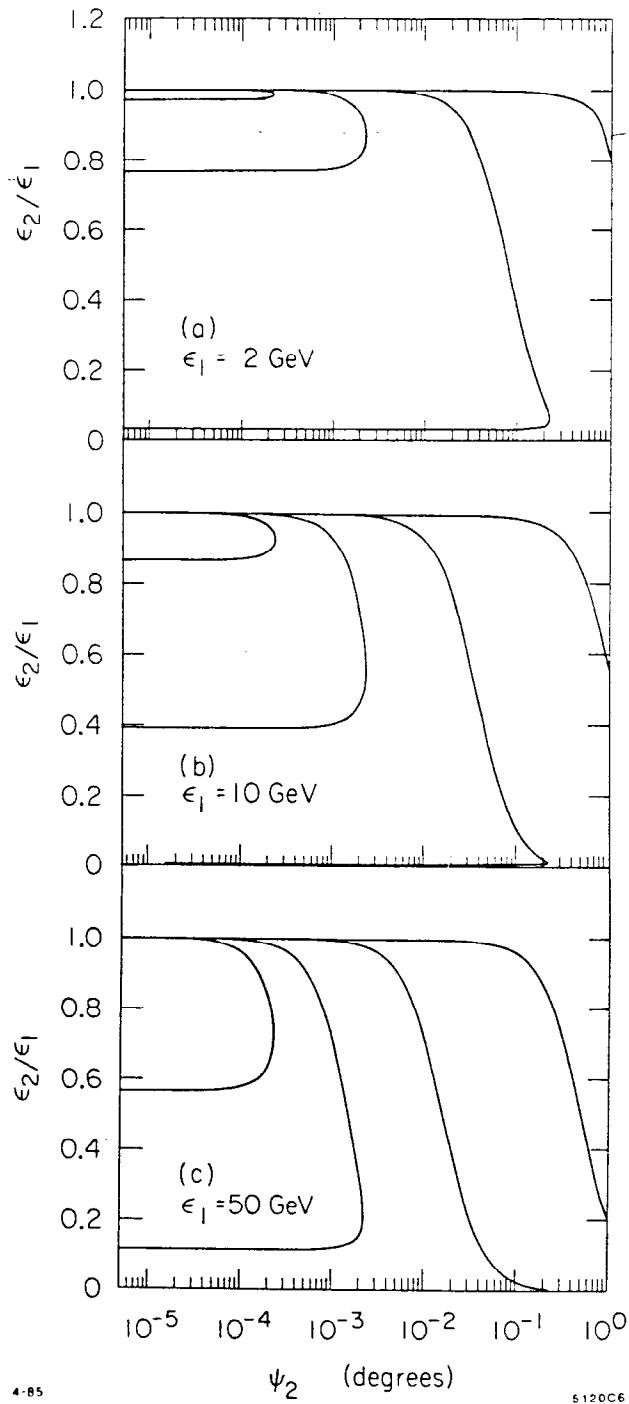


Fig. 5: Outgoing electron energy versus electron scattering angle corresponding to Fig's. 2 and 4.

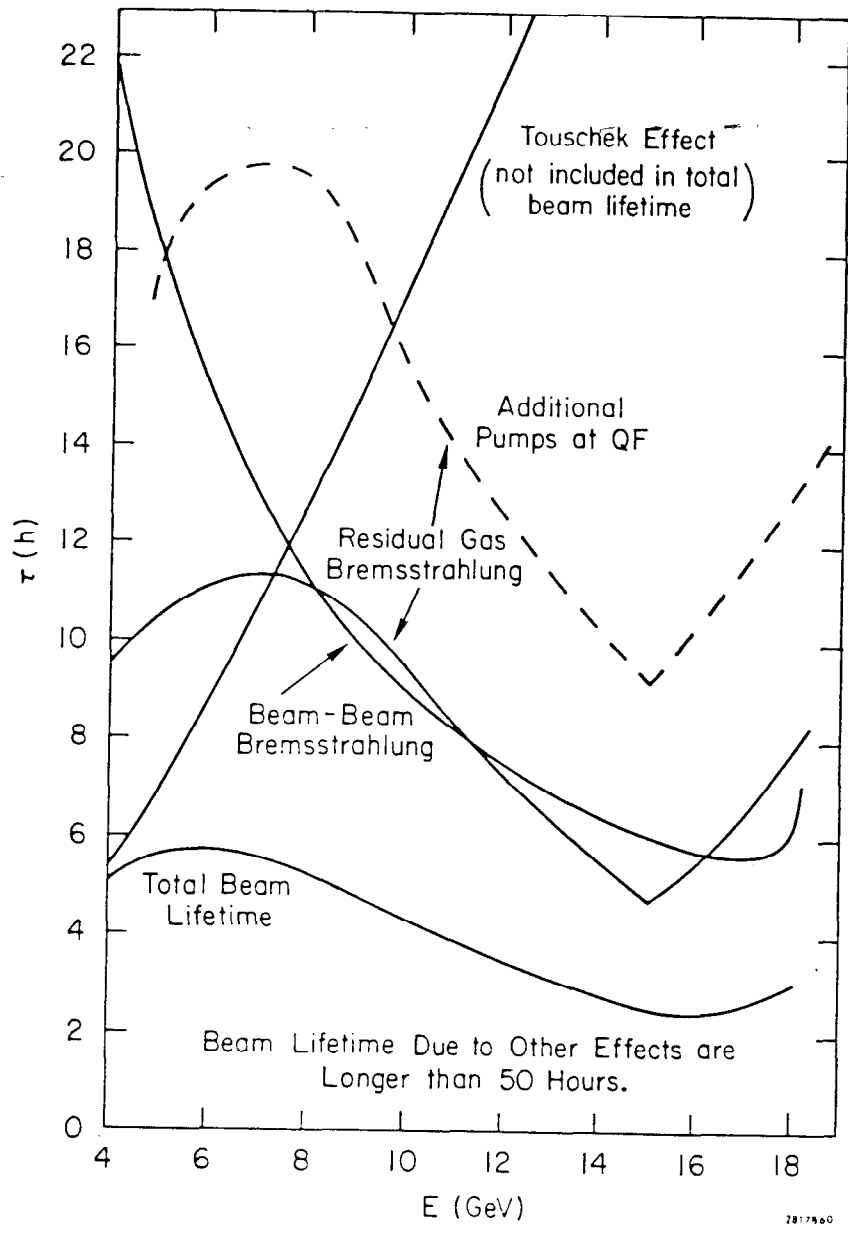


Fig. 6: Beam lifetime versus energy in PEP due to various effects.